

Dietrich Kohlheyer · Geert A. J. Besselink  
Rob G. H. Lammertink · Stefan Schlautmann  
Sandeep Unnikrishnan · Richard B. M. Schasfoort

## Electro-osmotically controllable multi-flow microreactor

Received: 27 April 2004 / Accepted: 28 October 2004 / Published online: 8 April 2005  
© Springer-Verlag 2005

**Abstract** An adjustable diffusion-based microfluidic reactor is presented here, which is based on electro-osmotic guiding of reagent samples. The device consists of a laminar flow chamber with two separate reagent inlets. The position and the width of the two sample streams in the flow chamber can be controlled individually by changing the flow ratio of three parallel guiding buffer streams. Since electro-osmotic flow (EOF) is used for pumping, no external pumps or other moving parts are needed. The region where the diffusive profiles of the two sample streams overlap is used for the reactions. This overlapping region can be manipulated in a predictable way by adjusting the voltages required to generate the respective electro-osmotic flow. Reaction dynamics inside the microreactor is illustrated with a reactant pair of a fluorescent calcium tracer and a calcium chloride solution. An analytical model, which is an analogue of electrical circuits to EOF, was developed and embedded into the LabView control software, allowing real-time control of the microreactor. This paper describes the simulation, fabrication and experimental characterisation of the device.

**Keywords** Microreactor · Microfluidics · Electro-osmotic flow · Address flow ·  $\mu$ TAS

### 1 Introduction

In the last decade, the research and development of microfluidic systems have grown rapidly, allowing the fabrication of “micro total analysis systems” ( $\mu$ TAS) or

“lab-on-a-chip” devices using technologies from the microelectronics industry (Northrup et al. 2003; Haswell and Skelton 2000). These microfluidic systems profit from their small dimension and high surface-to-volume ratios, allowing reaction and analysis to be fast and efficient (Fletcher et al. 1999; Haswell et al. 2001; Tudos et al. 2001). Furthermore, the energy and sample consumption in microfluidic structures are much lower compared to that in traditional macrofluidic systems. Flow in microfluidic channels is always laminar because of low Reynolds numbers (Brody et al. 1996), which makes it possible to have parallel flow streams without turbulent mixing (Weigl and Yager 1997). In such systems, transversal mass transport is based on diffusion. Micro total analysis systems include several passive and active microfluidic components, such as mixers and reactors. Microreactors integrated in such systems have been developed in different shapes, among which, the T-reactor is a well-known example (Haswell and Skelton 2000; Weigl and Yager 1997; Baroud et al. 2003; Yunus et al. 2002). The mixing of two homogeneous solutions in a T-reactor (with uniform zeta potential) and laminar flow is based only on diffusion. To influence the reaction yield, it is possible to vary, for instance, the concentrations of the reagent streams. In some applications, it might be of interest to control the extent of mixing, and, therefore, the reaction yield in a simpler way. The microreactor presented here is an adjustable diffusion-based one, which is easy to operate and fulfills these requirements. Fluid flow in this reactor is induced by electro-osmotic flow (EOF), which is a simple technique used for pumping aqueous solutions through microchannels. The major advantage of using EOF is that no external pumps or other moving parts are needed. Furthermore, EOF is easy to implement and operate, especially when more miniaturised structures are involved. More complex electro-osmotic fluid control became possible with the introduction of the FlowFET, an electro-osmotic pumping and switching device (Schasfoort et al. 1999). Here, we report on the design and evaluation of a microfluidic reactor driven by EOF.

D. Kohlheyer · G. A. J. Besselink · R. G. H. Lammertink  
S. Schlautmann · S. Unnikrishnan · R. B. M. Schasfoort (✉)  
Biochip Group, MESA+ Research Institute,  
Faculty of Science and Technology,  
University of Twente, P.O. Box 217,  
7500 AE Enschede, The Netherlands  
E-mail: r.b.m.schasfoort@utwente.nl  
Tel.: +31-53-4895621

## 1.1 Functional principle

In lab-on-a-chip devices, flow control is one of the most relevant issues. Electrokinetic control is a common technique used to adjust the width and the position of a sample plug, for instance, in capillary electrophoresis (Lin et al. 2002; Sinton et al. 2003). Methods for controlling the position of streams (hydrodynamically induced) using parallel guiding streams in a laminar-flow chamber has been demonstrated previously (Knight et al. 1998; Lee et al. 2001; Dittrich and Schwille 2003). The idea of address flow (Besselink et al. 2004) is to control both the position and the width of one central fluid stream (containing sample or reagent) entering a microfluidic chamber sandwiched by two parallel guiding streams. In address-flow devices, only EOF is used as the pumping technique. The position and width of the sample stream can be controlled by varying the flow ratio of the sample stream, as well as the guiding streams. This is done by adjusting the EOF voltage settings for the streams individually. Address flow is only possible in microsystems where turbulent mixing is absent. Since the chips contain no moving parts, the manufacturing becomes simpler. An analogue model of EOF to electrical circuits has been developed and embedded into a LabView program for real-time control during experimental work. Measurements were found to correspond well with the respective model (Besselink et al. 2004). To investigate the possibilities of controlling multiple sample streams inside a laminar-flow chamber, a two-sample address-flow chip has been developed. It has two sample streams and three guiding streams (Fig. 1). Both sample streams can be individually controlled in position and width by adjusting the EOF voltages according to the analytical model.

This two-sample address-flow chip is used as a microreactor. The reaction occurs where the diffusive profiles of the two reagent streams overlap (Fig. 2).

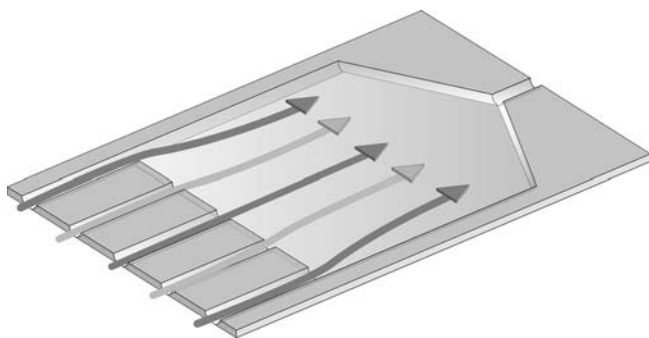


**Fig. 1** Illustration of the two-sample address-flow chip. The position and the width of two inner sample streams (second and fourth arrows) can be influenced in a predictable way with the adjustment of three parallel guiding streams (first, third and fifth arrows)

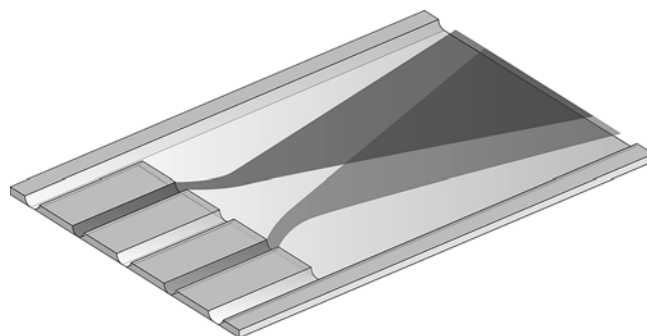


**Fig. 2** Illustration of the two-sample address-flow chip used as a microreactor. The region where the diffusive profiles of the two analyte streams overlap is used for reactions

## 2 Experimental methods

### 2.1 Microfabrication

The microfluidic chips were fabricated at the MESA<sup>+</sup> cleanroom facilities (Enschede, The Netherlands). Each chip consists of two glass plates: the top plate contains the channel structures, flow chamber and the reservoir holes, while the bottom plate is unprocessed. Processing of the top plate was done as follows: a 100 mm Pyrex glass wafer (Corning 7740) was coated with 1  $\mu\text{m}$  of amorphous silicon. After a standard lithography step, this silicon layer was structured by  $\text{SF}_6$  reactive ion etching. The silicon layer served as a mask during the following wet-etching step in 10% HF to create the channel and chamber structures in the underlying glass layer. For the inlet and outlet reservoirs, a second photolithography step was carried out on the backside using Ordyl BF410 resist foil. This foil was exposed to a UV light source and was developed in a sodium carbonate solution. After that, powder blasting was performed with  $\text{AlO}_3$  particles (30  $\mu\text{m}$  particle diameter) (Wensink and Elwenspoek 2002) to create the inlet and outlet holes. After ultrasonic cleaning in acetone and the removal of the silicon layer in 25% KOH, the wafer was chemically/mechanically polished, preparing the surface for the following fusion bonding step (Fan and Harrison 1994). Fusion bonding of the structured wafer to another Pyrex wafer was performed at 600°C. The bonded wafers were finally diced into several microfluidic chips. Figure 3 shows the design of the two-sample address-flow chip and Fig. 4 exhibits a chip manufactured from Pyrex glass according to that design.

### 2.2 Stream and reaction visualisation

The visualisation of streams and reactions was done using fluorescence microscopy. Bovine serum albumin (BSA) was obtained from Sigma (St. Louis, MO, USA). BSA was fluorescently labelled by treating with (a 60-fold molar excess of) fluorescein isothiocyanate in 0.5 M sodium borate, pH 9.0, for 30 min at room temperature,

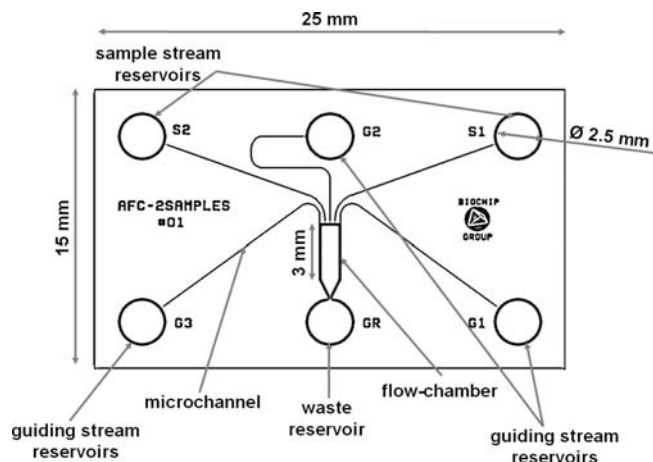


**Fig. 3** Design of a two-sample address-flow chip that was used for cleanroom fabrication. The chip dimensions are 15×25 mm. The chamber is 1,200 μm wide and 3 mm long. The width of the three guiding stream channels is 100 μm and the width of the two sample stream channels is 50 μm. Channel and chamber height is 10 μm

followed by gel filtration over a PD-10 column. Fluo-4 pentapotassium (salt, fluorescent calcium probe F14240) was obtained from Molecular Probes (Europe BV, Leiden, The Netherlands). Hepes buffer was obtained from Merck KGaA (Darmstadt, Germany). All the other chemicals were purchased from VWR International GmbH (Darmstadt, Germany) and were of analytical grade.

The two-sample address-flow chip was placed in an in-house-manufactured holder. This holder contains six reservoirs with integrated platinum electrodes connected to two high-voltage sources (IBIS 411, microfluidic control unit, IBIS Technologies B.V., Hengelo, The Netherlands). The applied voltages were controlled with a LabView (LabView 7.0, National Instruments) program based on the analytical model described below. An inverted (epifluorescence) microscope (Olympus IX51) with a UV light source and filter (U-MWB2 Wide-band

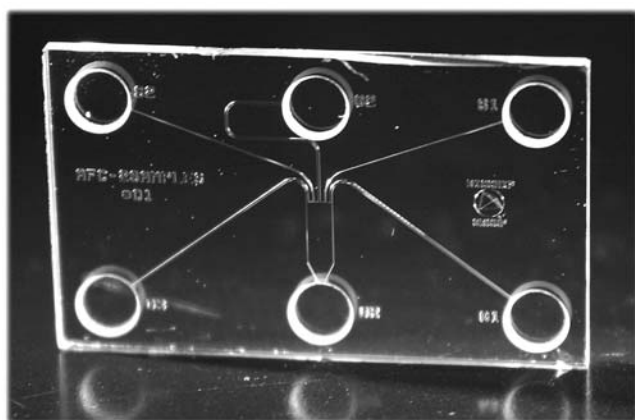


**Fig. 4** Photograph of the two-sample address-flow chip fabricated from Pyrex glass. The size of the chip is 15×25 mm

450–480 500 > 515, Olympus), equipped with an F-View II 12-bit digital camera (Soft Imaging System GmbH, Münster, Germany), was used. The camera control software AnalySIS (Soft Imaging System GmbH) was used to capture images and for the measurements of stream positions and widths.

The glass chips were thoroughly cleaned in 1 M NaOH and then rinsed with demineralized water to ensure reproducible surface characteristics. Before filling, the chip was rinsed with ethanol and dried with nitrogen. All inlet reservoirs were filled with 10 mM Hepes in demineralized water (adjusted with 0.1 M NaOH to pH 7.2). The Hepes buffer was chosen because of its low electrical conductivity, to minimise the effect of Joule heating. To remove air bubbles from the channels and the chamber, a vacuum was applied to the reservoirs by using a syringe. In the first experiment, fluorescently labelled BSA (7.5 μM in 10 mM Hepes buffer) was added as a stream marker to both sample stream reservoirs. To study reaction dynamics, the calcium indicator fluo-4 (50 μM fluo-4 in 10 mM Hepes buffer, supplemented with 1 mM EDTA to bind free Ca<sup>2+</sup> present as contamination) was added to the reservoir of one of the sample streams and a calcium solution (10 mM CaCl<sub>2</sub> in 10 mM Hepes buffer) to the other.

### 3 Results and discussion

#### 3.1 Analytical model

An analytical model was developed for calculating the required EOF potential settings to obtain the desired inlet flows. The developed model is based on an analogy of EOF to electrical circuits (Ajdari 2004; Qiao and Aluru 2002). It was developed just to show the possibility of adjusting the position and width of the reactant streams individually by controlling only the applied voltages, thereby, providing complete control over the reaction (zone). It is assumed that the parameters like electrical conductivity and fluid viscosity are homogeneous across the entire structure. The flow in the entire structure is driven only electro-osmotically. Since there is no pressure difference applied across this structure, this Ohmic model analogy takes only the electrical field across the structure into consideration for flow rate calculations. It can be concluded that the velocity at the chamber entrance is different from the velocity after the flow stabilises, owing to the non-uniform electrical field at the chamber entrance. It is obvious that these entrance effects cannot be completely removed. In order to simplify the calculations, entrance effects of the streams are neglected and it is assumed that the chamber velocity is uniform over the entire flow chamber.

Figure 5 shows a schematic drawing of the two-sample address-flow chip with all relevant geometrical and flow parameters. In order to determine the EOF potential settings, it is necessary to know the corre-

sponding channel and chamber fluxes. Owing to mass conservation, the total flux  $\Phi_{\text{ch}}$  inside the chamber is always the sum of the fluxes through the inlet channels:

$$\Phi_{\text{ch}} = u_{\text{ch}} A_{\text{ch}} = \sum_{i=1}^5 \Phi_i \quad (1)$$

where  $u_{\text{ch}}$  is the flow velocity inside the flow chamber and  $A_{\text{ch}}$  is the cross-section of the rectangular part of the flow chamber. For clarity in calculations, each channel is identified using an index  $i$ . It is possible to calculate each incoming flux  $\Phi_i$  as a fraction of the total flux  $\Phi_{\text{ch}}$  by determining the ratio of the corresponding stream widths  $W_{\text{ich}}$  (inside the chamber) to the total width of the flow chamber  $W_{\text{ch}}$ :

$$\Phi_i = \frac{W_{\text{ich}}}{W_{\text{ch}}} \Phi_{\text{ch}} \quad (2)$$

The stream widths  $W_{\text{ich}}$  depend on the positions ( $X_2$ ,  $X_4$ ) and the widths ( $W_{2\text{ch}}$ ,  $W_{4\text{ch}}$ ) of the two sample streams. Therefore, it is possible to replace the  $W_{\text{ich}}$  in Eq. 2 with the known parameters  $X_2$ ,  $X_4$ ,  $W_{2\text{ch}}$  and  $W_{4\text{ch}}$ :

$$\Phi_1 = \frac{x_2 - (W_{2\text{ch}}/2)}{w_{\text{ch}}} \Phi_{\text{ch}} \quad (3)$$

$$\Phi_2 = \frac{W_{2\text{ch}}}{w_{\text{ch}}} \Phi_{\text{ch}} \quad (4)$$

$$\Phi_3 = \frac{x_4 - x_2 - (w_{2\text{ch}}/2) - (w_{4\text{ch}}/2)}{w_{\text{ch}}} \Phi_{\text{ch}} \quad (5)$$

$$\Phi_4 = \frac{W_{4\text{ch}}}{w_{\text{ch}}} \Phi_{\text{ch}} \quad (6)$$

$$\Phi_5 = \frac{w_{\text{ch}} - x_4 - (w_{4\text{ch}}/2)}{w_{\text{ch}}} \Phi_{\text{ch}} \quad (7)$$

For further calculations of the electrical voltages, the fluidic network (the channels and the chamber) has to be replaced by its analogous electrical resistance, as shown in Fig. 6. Since the flow in the inlet channels is induced electro-osmotically, the flux depends on the applied electrical field and the electro-osmotic mobility, according to the Helmholtz–Smoluchowski equation:

$$\Phi_i = u_i A_i = \mu_{\text{EOF}i} E_i A_i = \mu_{\text{EOF}i} \frac{V_i - V_{\text{ch}}}{L_i} A_i \quad (8)$$

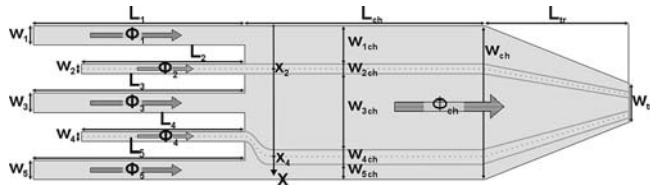


Fig. 5 Schematic drawing of the two-sample address-flow chip with corresponding parameters

where  $u$  is the fluid velocity,  $A$  the cross-section of the channel,  $\mu_{\text{EOF}}$  the electro-osmotic mobility,  $E$  the electric field,  $L$  the length of the channel,  $V$  the applied voltage at an inlet reservoir and  $V_{\text{ch}}$  the electrical potential at the entrance to the flow chamber.

For simplification, it was assumed that the electrical field at the flow-chamber entrance is uniform (as displayed in Fig. 6 by the junction of the five resistors). For a straight channel of length  $L$ , cross-section  $A$  and which is filled with a solution of electrical conductivity  $\sigma$ , the electrical resistance is given by:

$$R_i = \frac{L_i}{\sigma A_i} \quad (9)$$

And for the flow chamber with its rectangular part (length  $L_{\text{ch}}$  and cross-section  $A_{\text{ch}}$ ) and trapezoid part (length  $L_{\text{tr}}$  and outlet cross-section  $A_{\text{tr}}$ ), the electrical resistance is given by:

$$R_{\text{ch}} = \underbrace{\frac{L_{\text{ch}}}{\sigma A_{\text{ch}}}}_{\text{rectangular}} + \underbrace{\frac{L_{\text{tr}}}{\sigma (A_{\text{ch}} - A_{\text{tr}})} \ln \left( \frac{A_{\text{ch}}}{A_{\text{tr}}} \right)}_{\text{trapezoid}} \quad (10)$$

To calculate the voltage drop across the channels ( $V_i - V_{\text{ch}}$ ) and, thereby, the flux in each channel, the electrical potential  $V_{\text{ch}}$  has to be calculated first. This can be obtained by calculating the total current in the chamber  $I_{\text{ch}}$ :

$$\begin{aligned} I_{\text{ch}} &= \sum_{i=1}^5 I_i \Rightarrow \frac{V_{\text{ch}}}{R_{\text{ch}}} = \sum_{i=1}^5 \frac{V_i - V_{\text{ch}}}{R_i} \\ \Rightarrow V_{\text{ch}} &= R_{\text{ch}} \sum_{i=1}^5 \frac{V_i - V_{\text{ch}}}{R_i} \end{aligned} \quad (11)$$

With Eqs. 8 and 11, it is now possible to calculate  $V_{\text{ch}}$  as follows:

$$V_{\text{ch}} = \frac{R_{\text{ch}}}{\mu_{\text{EOF}i}} \sum_{i=1}^5 \frac{\Phi_i L_i}{R_i A_i} \quad (12)$$

Finally, from Eqs. 8 and 12,  $V_i$  can be deduced:

$$V_i = \frac{\Phi_i L_i}{A_i \mu_{\text{EOF}i}} + \frac{R_{\text{ch}}}{\mu_{\text{EOF}i}} \sum_{j=1}^5 \frac{\Phi_j L_j}{R_j A_j} \quad (13)$$

Using Eq. 13, it is possible to calculate all five voltages needed to obtain any desired regime of positions, widths and velocities of the two sample streams.

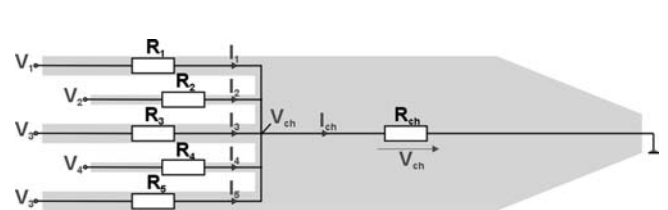
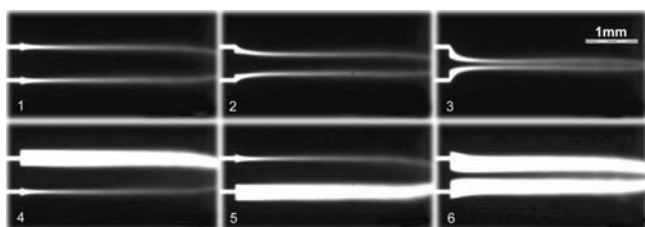


Fig. 6 Electrical circuit for a two-sample address-flow chip

### 3.2 Experimental results

Figure 7 shows images of the two-sample address-flow device working under different guiding potential settings. The positions and widths of the sample streams were changed, keeping the velocity inside the flow chamber constant (750  $\mu\text{m/s}$ ). It can be observed in the top three images (1, 2 and 3 in Fig. 7) that the distance between the two sample streams was reduced from 625  $\mu\text{m}$  to 10  $\mu\text{m}$ , whilst maintaining the widths of both sample streams at 50  $\mu\text{m}$ . In image 4 of Fig. 7, the width of sample stream 1 was set to 200  $\mu\text{m}$  and that of sample stream 2 to 50  $\mu\text{m}$ . In image 5 of Fig. 7, the width of sample stream 1 was set to 50  $\mu\text{m}$  and that of sample stream 2 to 200  $\mu\text{m}$ . In image 6 of Fig. 7, both streams were set to widths of 200  $\mu\text{m}$  and the distance between the two streams was set to 50  $\mu\text{m}$ . Confirmation of the chamber velocity was performed by using a conventional stopwatch measurement technique. Stream positions and widths (full-width-half-maximum method) were measured using the AnalySIS software.

When reacting components are added to the sample stream reservoirs, the two-sample address-flow chip can be used as a microreactor. By adjusting the positions and the widths of the two sample streams, the overlapping region (reaction zone) of the diffusive reagent profiles can be adjusted. To illustrate that the two-sample address-flow chip can be used as a microreactor, the following experiment was performed. First, the chip was completely filled with the buffer solution. After that, one sample stream reservoir was emptied and refilled with fluo-4 (a calcium indicator). The other sample stream reservoir was filled with the  $\text{CaCl}_2$  solution. The flow velocity in the chamber was set to 250  $\mu\text{m/s}$ . After binding with calcium, fluo-4 will strongly increase its fluorescence. The fluorescence of the calcium indicator was measured with the microscope setup described in Sect. 2.2. Figure 8 shows a picture series of images, which were taken during the experiment. It can be observed that the reaction yield (fluo-4/ $\text{Ca}^{2+}$  complex) became higher as the distance between the two sample streams was consistently reduced. Also, it can be seen that the overlapping reaction region is asymmetric. This is owing to the difference between the diffusive profiles



**Fig. 7** Images obtained with a digital camera attached to the fluorescence microscope showing different stream positions and widths of the two sample streams visualised with fluorescently labelled BSA. The flow direction is from left to right (velocity  $u_{\text{ch}} \approx 750 \mu\text{m/s}$ )

of the fluo-4 (diffusion coefficient  $D_{\text{fluo-4}} \approx 2 \times 10^{-10} \text{m}^2/\text{s}$ , (Song et al. 2003) and the calcium (diffusion coefficient  $D_{\text{Ca}^{2+}} \approx 1.6 \times 10^{-9} \text{m}^2/\text{s}$ , Song et al. 2003) reactant streams. In the reaction zone, mixing is dominated by the diffusion of  $\text{Ca}^{2+}$ , which is smaller than fluo-4 and was used in excess. It can also be observed in Fig. 8 that the fluo-4 indicator stream exhibits a background fluorescence when entering the reaction chamber. This might be due to contamination of undesired calcium in the buffer solution or due to autofluorescence of the unbound fluo-4 molecules.

### 3.3 Simulations

In addition to the experiments, the presented microfluidic structure was simulated using the software package CFDRC (CFD Research Corporation, Huntsville, AL, USA). For a chemical reaction, it could be of interest to be able to vary the reaction yield without changing the reactant concentrations or flow velocity in the reaction chamber. The following simulation was performed to show the possibility of stabilising the reaction yield, even in the case of a fluctuating reactant concentration, by adjusting the positions and widths of the reactant streams.

In this simulation, the overlapping region of the two diffusive sample streams (both containing the same sample with a diffusion coefficient  $D = 1 \times 10^{-8} \text{m}^2/\text{s}$ ) was studied for different positions and widths (of the two sample streams). This was done by calculating the variation of the concentration along the centreline of the overlapping region. The microfluidic device was approximated as a two-dimensional structure with approximately 7,000 grid cells. The simulation was performed with “no-slip conditions at walls.” The electrical boundary conditions were obtained from the analytical model. Both sample streams were programmed to contain an equivalent concentration of sample and to have a width of approximately 100  $\mu\text{m}$ . The electro-osmotic mobility was set to  $5 \times 10^{-8} \text{m}^2/\text{V}$  for all guiding, and sample, streams. An overlapping region between the two sample streams was established at a velocity of 400  $\mu\text{m/s}$  in the flow chamber. Figure 9

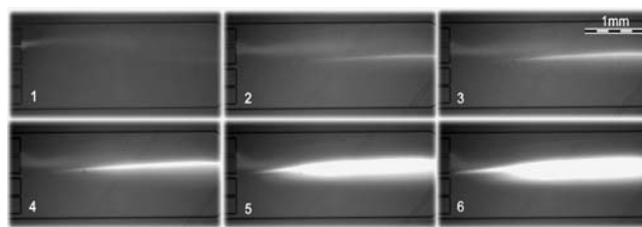
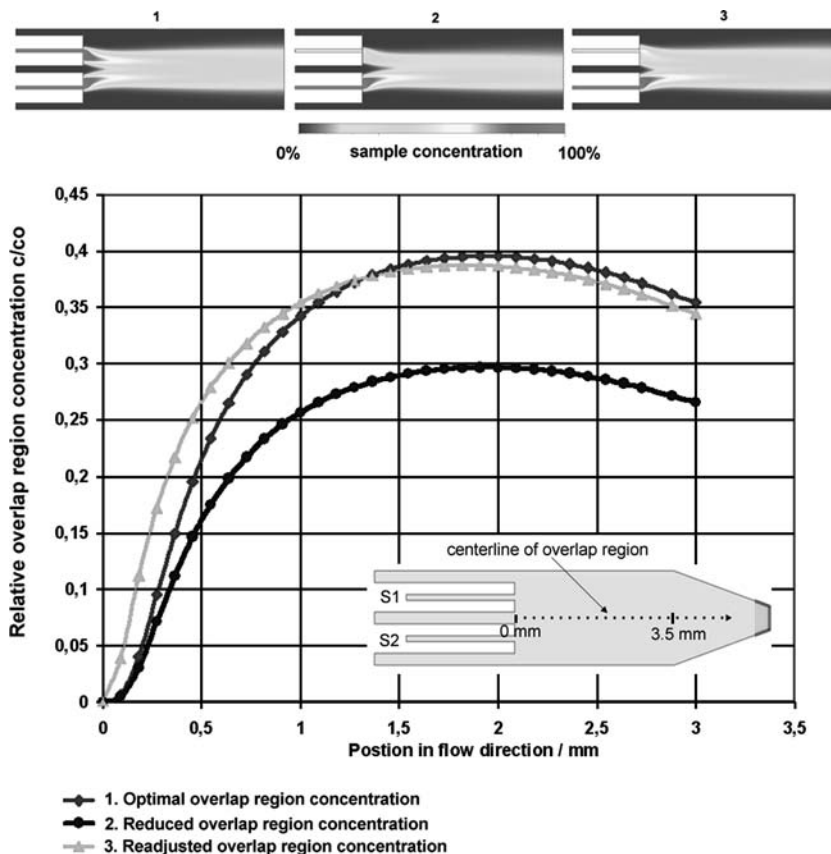


**Fig. 8** Fluorescence microscope images showing different intensities of the reaction product fluo-4/ $\text{Ca}^{2+}$ . From images 1 to 6, a decrease of distance between the two reactant streams results in an increasing yield of the fluo-4/ $\text{Ca}^{2+}$  complex. The flow direction is from left to right (velocity  $u_{\text{ch}} \approx 250 \mu\text{m/s}$ )

**Fig. 9** Diagram showing three overlapping region concentration profiles obtained from CFDRC simulation. Line 1 shows the optimal concentration with two identical streams. Line 2 represents the concentration after reducing the inlet concentration of stream 1 to 50% of its original value. Line 3 represents the concentration after adjusting the width and position of stream 1 to achieve a similar concentration as in line 1. The respective stream positions and their concentrations can be seen in the top three images



illustrates three curves representing concentration profiles along the centreline of the overlapping region (in the flow direction) during the simulation. Line 1 in Fig. 9 shows the optimal concentration profile that results in case of two identical streams (same width and concentration). Then, the concentration of sample stream 1 was reduced to 50% of the original value while the concentration of sample stream 2 was left unchanged. The decreased sample concentration in the first sample stream causes a drop of the concentration in the overlapping region (Fig. 9, line 2) to 75% of the previous value. By changing only the width and the position of the first sample stream, a new concentration profile was established that closely resembles the optimal concentration profile (Fig. 9, line 3).

### 3.4 Conclusions

An adjustable diffusion-based microfluidic reactor has been designed and successfully fabricated. Electro-osmotic flow (EOF) is used as a pumping technique inside the channels. For this reason, no external pumps or other sophisticated systems are needed. Experimental and simulation results showed that the reaction yield could be manipulated by controlling the EOF potential settings. This device allows us to adjust the reaction yield inside the reaction chamber, even in the case of fluctuating reactant concentrations. Since the

ratio of all inlet flows is always proportionally varied, the flow rate inside the reaction chamber remains constant while the reaction yield is manipulated. Furthermore, an analytical model based on an electrical circuit has been developed and tested. This model makes it possible to control the position and width of reagent streams in real time and in a predictable way. The chip can be used as a new component for upcoming lab-on-a-chip or micro total analysis systems ( $\mu$ TAS) technology.

**Acknowledgements** The authors would like to acknowledge the funding of this research by the “Netherlands Organization for Scientific Research” (NWO) as a part of the SPRINTLOC “Vernieuwings-impuls” project.

### References

- Ajdari A (2004) Steady flows in networks of microfluidic channels: building on the analogy with electrical circuits. *C R Phys* 5:539–546
- Baroud CN, Okkels F, Ménétrier L, Tabeling P (2003) Reaction–diffusion dynamics: Confrontation between theory and experiment in a microfluidic reactor. *Phys Rev E* 67:060104
- Besselink GAJ, Vulto P, Lammertink RGH, Schlautmann S, van der Berg A, Olthuis W, Engbers GHM, Schasfoort RBM (2004) Electroosmotic guiding of sample flows in a laminar flow chamber. *Electrophoresis* 25:3705–3711
- Brody JP, Yager P, Goldstein RE, Austin RH (1996) Biotechnology at low Reynolds numbers. *Biophys J* 71:3430–3441

- Dittrich PS, Schulle P (2003) An integrated microfluidic system for reaction, high-sensitivity detection, and sorting of fluorescent cells and particles. *Anal Chem* 75:5767–5774
- Fan ZH, Harrison DJ (1994) Micromachining of capillary electrophoresis injectors and separators on glass chips and evaluation of flow at capillary injections. *Anal Chem* 66:177–184
- Fletcher PDI, Haswell SJ, Paunov VN (1999) Theoretical considerations of chemical reactions in micro-reactors operating under electroosmotic and electrophoretic control. *Analyst* 124:1273–1282
- Haswell SJ, Skelton V (2000) Chemical and biochemical microreactors. *Trends Anal Chem* 6:389–395
- Haswell SJ, Middleton RJ, O'Sullivan B, Skelton V, Watts P, Styring P (2001) The application of micro reactors to synthetic chemistry. *Chem Commun* 5:391–398
- Knight JB, Vishwanath A, Brody JP, Austin RH (1998) Hydrodynamic focusing on a silicon chip: mixing nanoliters in microseconds. *Phys Rev Lett* 80:3863–3866
- Lee GB, Hwei BH, Huang GR (2001) Micromachined pre-focused M×N flow switches for continuous multi-sample injection. *J Micromech Microeng* 11:654–661
- Lin JY, Fu LM, Yang RJ (2002) Numerical simulation of electrokinetic focusing in microfluidic chips. *J Micromech Microeng* 12:955–961
- Northrup MA, Jensen KF, Harrison DJ (2003) *Micro total analysis systems 2003*. Kluwer, Dordrecht, The Netherlands
- Quiao R, Aluru NR (2002) A compact model for electroosmotic flows in microfluidic devices. *J Micromech Microeng* 12:625–635
- Schasfoort RBM, Schlautmann S, Hendrikse J, van den Berg A (1999) Field effect flow control for microfabricated fluidic networks. *Science* 286:942–945
- Sinton D, Ren L, Li D (2003) A dynamic loading method for controlling on-chip microfluidic sample injection. *J Colloid Interface Sci* 266:448–456
- Song H, Bringer MR, Tice JD, Gerdtz CJ, Ismagilov RF (2003) Experimental test of scaling of mixing by chaotic advection in droplets moving through microfluidic channels. *Appl Phys Lett* 83:4664–4666
- Tudos AJ, Besselink GAJ, Schasfoort RBM (2001) Trends in miniaturized total analysis systems for point-of-care testing in clinical chemistry. *Lab on a Chip* 1:83–95
- Weigl BH, Yager P (1997) Silicon-microfabricated diffusion-based optical chemical sensor. *Sensors Actuators B* 39:425–457
- Wensink H, Elwenspoek MC (2002) Reduction of sidewall inclination and blast lag of powder blasted channels. *Sensors Actuators A* 102:157–164
- Yunus K, Marks CB, Fisher AC, Allsopp DWE, Ryan TJ, Dryfe RAW, Hill SS, Roberts EPL, Brennan CM (2002) Hydrodynamic voltammetry in microreactors: multiphase flow. *Electrochim Commun* 4:579–583